Robustness and perturbation in the modeled cascade heart rate variability

D. C. Lin

Department of Mechanical, Aerospace and Industrial Engineering, Ryerson University, Toronto, Ontario, Canada M5B 2K3

(Received 3 July 2002; revised manuscript received 8 November 2002; published 24 March 2003)

In this study, numerical experiments are conducted to examine the robustness of using cascade to describe the multifractal heart rate variability (HRV) by perturbing the hierarchical time scale structure and the multiplicative rule of the cascade. It is shown that a rigid structure of the multiple time scales is not essential for the multifractal scaling in healthy HRV. So long as there exists a tree structure for the multiplication to take place, a multifractal HRV and related properties can be captured by using the cascade. But the perturbation of the multiplicative rule can lead to a qualitative change. In particular, a multifractal to monofractal HRV transition can result after the product law is perturbed to an additive one at the fast time scale. We suggest that this explains the similar HRV scaling transition in the parasympathetic nervous system blockade.

DOI: 10.1103/PhysRevE.67.031914 PACS number(s): 87.19.Hh, 89.75.Da

I. INTRODUCTION

The dynamics of the cardiovascular regulation is highly irregular in most physiological conditions, a phenomenon commonly referred to as the heart rate variability (HRV). Captured in the interbeat time RR interval (RRi) (interbeat time is defined by the timespan of the successive R waves in the electrocardiogram), HRV reveals mostly the fluctuating autonomicity at the sinoatrial node. This fluctuation is believed to give rise to a *fractal component* of HRV that contributes to the $1/f$-like RRi power spectrum [1–5]. Similar to other $1/f$ phenomena in nature, the fractal component of HRV represents a very robust feature that has been observed in different body positions [1,2], the times of day [3], and the health conditions [2,4]. While its physiological origin and purpose remain largely unknown, the fractal HRV has drawn much interest in recent years for a number of reasons. First, in healthy humans, the $1/f$ power can reach 70 to 90% of the total RRi signal power [1,2,4]. Furthermore, experimental data suggest potential clinical relevance as a diminishing fractal component was found to correlate well with a higher mortality rate in certain heart disease conditions [2,4,6]. Although such a correlation has only been systematically established for short-term HRV, fractal scalings in long-term recordings ($\sim 10^5$ beats) are known to be qualitatively different for healthy and diseased populations [7–10].

Recent studies indicated that the scaling in healthy RRi is in fact highly nonuniform. The possibility of a multifractal HRV was thus raised [8–10], and tested with encouraging results by using discrete multiplicative random cascade [9,10]. Using the cascade to model heart rate regulation provides an interesting contrast to the general notion of feedback which functions on the basis of additive law. A possible explanation for this result is that complex biological functions such as regulating the heart rate are achieved via the interaction of a large number of control mechanisms over a wide range of scales. Hence, one or few isolated reflexes are not sufficient to capture the overall complexity. For example, the reduction of baroreflex sensitivity and its recovery dynamics in prolong bed rest test exhibit qualitatively very different property from the long term HRV. Thus, baroreflex alone is insufficient to describe the complex HRV [14]. The encouraging result from the cascade model implies a multiplicative interaction in the autonomic heart rate controls. Similar phenomenology in natural systems, such as turbulence [15], network traffic [16], and market dynamics [17] further suggests the product law may exist on a more general ground.

Autonomic nervous system blockade is sufficient to alter the multifractal HRV in a fundamental way. It was shown a multifractal to monofractal transition (MMFT) in the parasympathetic nervous system (PNS) blockade, but not in sympathetic nervous system (SNS) blockade [11]; see also Ref. [12]. Because of the health implication of reduced HRV, it is plausible MMFT may also describe the transition to heart disease in such pathologic state as congestive heart failure where there is an elevated sympathetic drive and PNS withdrawal [2,4,13].

To further the cascade theory of HRV, it is necessary to consider different model configurations and HRV in other physiological conditions. This paper presents the research results on these issues. Specifically, we focus on the robustness of multifractal and the cause of MMFT by perturbing the cascade. There is a twofold objective for these investigations. The first is related to the proposition of cascade HRV itself. Granted the product law is a logical framework by which the multifractal HRV can be explained, discrete cascades are artificial in nature and lack the motivation in real physical or physiological terms. The study of the robust multifractal generation is an attempt to address this modeling issue. Our goal is to relax the artificiality in cascade and to test the limit of using the cascade paradigm to describe HRV. Specifically, numerical experiments will be conducted to perturb the hierarchical time scale structure and the multiplicative rule of the cascade to test the persistence of multifractal scaling. We will show that the arrangement of the multiple time scales in the discrete random cascade is not an essential factor. This result attests the omnipresence of multifractal objects in diverse physical systems in general, and lends hope for the physical basis of cascade HRV in particular. The study of the ''unstable'' multifractal generation leads to the second objective of the numerical study; namely, finding the cause of MMFT in the context of cascade. We will show that the random perturbations of the product rule into an additive one is sufficient to cause MMFT. It supports the early sug-

gestion that an additive law manifested by one or a few feedback mechanisms may not be sufficient to characterize complex biological functions such as regulating the heart rate.

This paper is organized into four sections. In Sec. II, we provide an overview for cascade HRV. We will demonstrate how cascade parameters can be extracted from RRi and compare the simulation results with experimental data. Certain technical issues related to the estimation of multifractal will also be addressed. In Sec. III, cascade perturbations are conducted to test the persistence and destruction of multifractal. The concluding remarks are given in Sec. V.

II. CASCADE HRV

The structure of the discrete random cascade can generally be put in the framework of positive martingale theory [18]. For numerical study, the construction of the cascade is defined by three basic elements (a) the (multiplicative) data generation rule, (b) the probability law for the cascade component, and (c) the branching rule. The cascade HRV proposes that the fractal component of HRV is a result of the product of $J+1$ random variables ω_j which we call cascade components

$$\tau_J(t)=\prod_{j=0}^{J}\omega_j(t), \tag{1}$$

where $\omega_j(t)=1+\xi_j$ and ξ_j, $j=0,...,J$ are independent (in j) random variables with $\langle\xi_j\rangle=0$, $\langle\xi_j\xi_{j'}\rangle=\delta_{jj'}\sigma_j^2$ ($\delta_{jj'}$ is the Kronecker delta). Equation (1) defines the data generation rule (a) and describes the mechanism for data fluctuation in the cascade. Gaussian $\omega_j(t)$'s will be used through out this study since the outcome of our results does not vary sensitively on this choice. Each $\omega_j(t)$ is set to vary at the integer times $\{t_k^{(j)},k,j\in\mathbb{N}\}$, $\omega_j(t)=\omega_j(t_k^{(j)})$ for $t_k^{(j)}\leqslant t<t_{k+1}^{(j)}$. The time sets $\{t_k^{(j)}\}$, $j=0,...,J$, define the branching rule (c) and the multiple time scales in the cascade.

The hypothesis of cascade HRV has led to an effective modeling strategy for HRV. Assuming a Gaussian *bounded* cascade with a dyadic branching rule $t_k^{(j)}=k\delta_j$, $k=0,...,2^j$ and $\delta_j=2^{J-j}$, HRV in health [9,10] and in autonomic nervous system blockades [10] have been successfully simulated. Assuming a bounded cascade is based on the electrophysiology of the heart muscle cells, which dictates a bounded RRi. Letting $\sigma_j=\sigma_0 2^{-\alpha(j-1)}\sim\delta_j^{\alpha}$, $j=1,...,J$, assures a bounded $r_J(t)$ in the $J\to\infty$ limit [10]; see also Ref. [19].

For large J, the estimation of α can be made by the log increment of the actual RRi data $\mathbf{r}(t)$: $\Delta\mathbf{y}(\tau,t)=\log_2[\mathbf{r}(t+\tau)]-\log_2[\mathbf{r}(t)]$. It can be shown that $\langle\Delta\mathbf{y}(\tau,t)^2\rangle\sim\tau^{2\alpha}$, where the angle brackets denote the statistical average over t (Appendix A). Figure 1 shows the averaged $\sqrt{\langle\Delta\mathbf{y}^2\rangle}$ from two databases: the first (DB1) consists of 10 sets of daytime RRi recording of normal sinus rhythm from healthy young adults and the second (DB2) consists of 18 sets of daytime RRi of normal sinus rhythm downloaded from the public domain physionet [20]. A scaling range for the group-averaged $\langle\Delta\mathbf{y}^2\rangle$ is found in $\tau>2^4$ beats and $\alpha\sim0.126$,

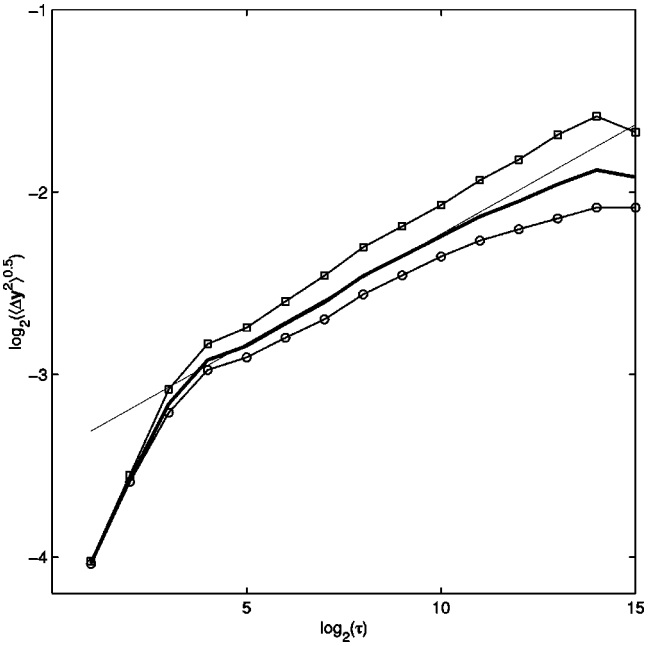

FIG. 1. $\log_2(\langle\Delta\mathbf{y}(r)^2\rangle^{0.5})$ vs $\log_2(\tau)$ based on real RRi data from DB1 (□) and DB2 (○). The heavy solid line is the overall average. The power law for σ_j is estimated with $\alpha=0.126$ and $\log_2(\sigma_0)=-1.6$ (at the intercept with the y axis at $J=15$). The thin solid line is the corresponding regression line given by $1.6+0.126\log_2(\tau)$.

$\log_2(\sigma_0)\sim-1.6$ (the intercept of the regression line at the largest τ value) can be estimated. Using this method, the generated cascade can mimic the experimental RRi property very well (Fig. 2). Note also from Fig. 1 that there appears to have a second range in $\tau<2^4$ with the estimated $\alpha\sim0.43$. This value corresponds to a scaling exponent ~1.86 for the power law spectrum, which is close to that of a Brownian motion and which reminds us of the ''cross-over'' phenomenon or double scaling in the literature of long-term HRV [7].

The multifractal analysis of the dyadic cascade HRV was conducted based on the moment of the absolute increment. For $r_j(t)$, we formed $\mathcal{S}_J(\tau,q)=\langle|\Delta r_J(\tau)|^q\rangle$, where $\Delta r_J(\tau)=r_J(t+\tau)-r_J(t)$ [9,10]. It can be shown that $\mathcal{S}_J(\tau,q)\sim\tau^{\gamma(q)}$ in large τ where $\gamma(q)$ is defined by

$$\left\langle\left|\prod_{i=1}^{j}\omega_i(t)\right|^q\left|\prod_{i=j+1}^{J}\omega_i(t+\tau)-\prod_{i=j+1}^{J}\omega_i(t)\right|^q\right\rangle\sim\delta_j^{\gamma(q)}. \tag{2}$$

If the variance σ_j of the cascade component decays sufficiently fast, the cascade in higher generations is approximately additive. As a result, a second scaling can emerge from the model in small τ: $\mathcal{S}_J(\tau,q)\sim\tau^{\alpha q}$ (Appendix B). Hence, the ''cross-over'' phenomenon mentioned above can be modeled by using two decay rates, i.e., for $1<p<J$ and $\alpha_1<\alpha_2$, one in $1\leqslant j\leqslant p$ with $\sigma_j=\sigma_0 2^{-\alpha_1(j-1)}$ and one in $p<j\leqslant J$ with $\sigma_j=\sigma_0 2^{-\alpha_2(j-1)}$ In this case, $\mathcal{S}_J(\tau,q)\sim\tau^{\alpha_2 q}$ for $\tau\leqslant 2^p$ and $\mathcal{S}_J(\tau,q)\sim\tau^{\gamma(q)}$ for $\tau>2^p$ (Fig. 3).

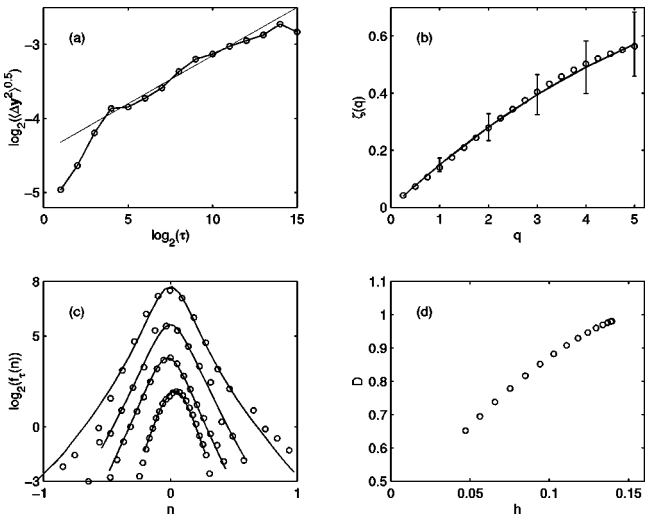

FIG. 2. Comparison between experimental and numerical $\zeta(q)$ function and increment PDF. (a) $\log_2(\langle \Delta \mathbf{y}(\tau)^2 \rangle^{0.5})$ vs $\log_2(\tau)$ from a typical data set in DB2 ($\bigcirc$) and the linear fit of the power law ($-$): $\log_2(\langle \Delta \mathbf{y}(\tau)^2 \rangle^{0.5}) = -2.5 - 0.13 \log_2(\tau)$. (b) Experimental ($\bigcirc$) and numerical ($-$) $\zeta(q)$s. (c) Experimental ($\bigcirc$) and numerical increment PDF ($-$) ($n = \Delta r_J$ or $\Delta \mathbf{r}$). For better comparison, $f_\tau(\Delta \mathbf{r})$ is rescaled horizontally and vertically by arbitrary factors f_0 and $1/f_0$, respectively. (d) The multifractal spectrum $D(h)$ of the experimental data (based on the Legendre transform $D(h) = \min_q [qh - \zeta(q) + 1]$). The numerical result is averaged over 100 samples of $r_J(t)$ with $\log_2(\sigma_j) = -2.5 - 0.13(j-1)$. Vertical bars at $q = 1,...,5$ show the standard error of the statistic.

For higher order moment $q \gg 1$, the dyadic bounded cascade predicts $\mathcal{S}_J(\tau,q) \sim \tau$ and $\zeta(q) = 1$. However, this property is difficult to verify from RRi due to the insufficient data length.

The estimated $\zeta(q)$ allows further calculations of the multifractal spectrum. Let $h = \zeta(q)' = d\zeta(q)/dq$ which measures the so-called singularity strength. The ''size'' of the set of increments for a given α, or its Hausdorff dimension $D(h)$, can be related to $\zeta(q)$ via a Legendre transform [21,22]

$$D(h) = \min_q [qh - \zeta(q) + 1].$$

It is known, for monofractal, that $\zeta(q) = qH$ describes a linear law and, for multifractal, a qualitatively different nonlinear $\zeta(q)$ with $\zeta(q)'' < 0$ results [23]. The typical multifractal spectrum for daytime HRV of a healthy young adult is shown in Fig. 2(c) for $q > 0$. Notice the maximum $D(h)$ is reached for $h \sim 0.15$.

To conclude this section, we would like to discuss some technical issues related to using $\mathcal{S}_J(\tau,q)$ for multifractal analysis. In the context of fluid turbulence, $\mathcal{S}_J(\tau,q)$ is nothing but the structure function of the absolute velocity increment. Although it was widely used in the past, the structure function is known to diverge for $q < 0$ since the probability at zero increment does not vanish. Moreover, as Muzy *et al.* pointed out, the structure function approach is limited in the range $h \in (0,h^*)$, where $h^* = 1 - [1 - D(h^*)]/D'(h^*) < 1$ [21]. This upper bound exists when $\max[D(h_m)]$ occurs at some $h_m > 1$. If $h_m < 1$, the accessible range becomes $h \in (0,1)$ for all $q > 0$ if and only if there is no negative singularity. If there exists a $q_* > 0$ where $h(q) < 0$, $q > q_*$, and $h_m < 1$, the accessible range is further restricted to $q < q_*$ (when $\zeta(q)$ begins to bend downward [$d\zeta(q)/dq < 0$]). As shown in Fig. 2(c), the typical range for long-term HRV is $h < 1$. Then, the potential concern lies in the negative h. We did observed $d\zeta(q)/dq < 0$ in the higher order moments ($q > 5$) from some daytime RRi data, and more often in nighttime RRi. For this reason, the multifractal scaling in large q has not been resolved by using this approach in the past [9,10]. Nevertheless, the qualitative feature of a nonlinear $\zeta(q)$ is already revealed for small q and $\mathcal{S}_J(\tau,q)$ will be used for the purpose of this study.

III. PERTURBED RANDOM CASCADE

Although the discrete cascade proposed in the past has been effective for modeling the fractal property of HRV, it is nonetheless artificial and therefore lacks the motivation in

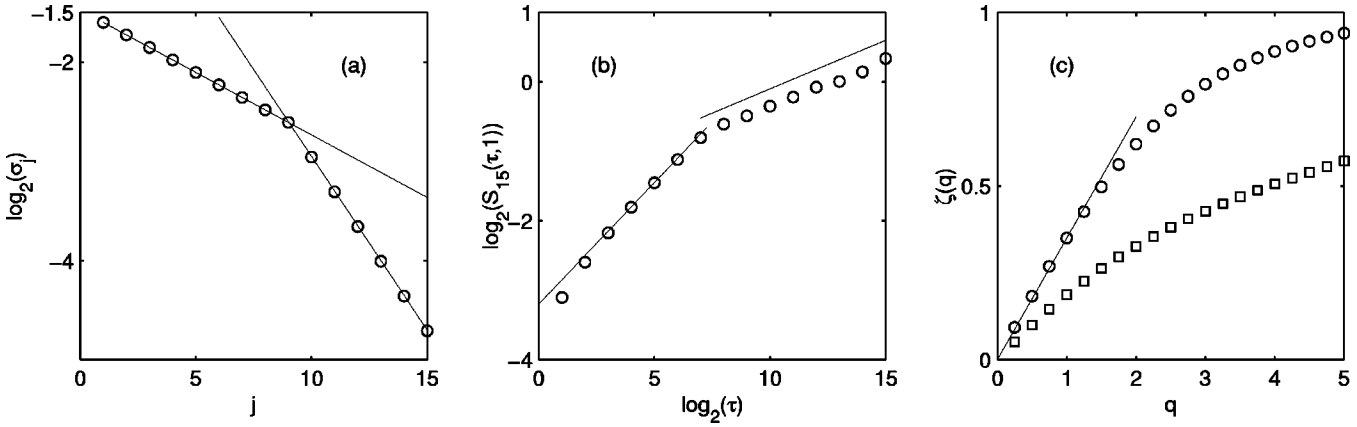

FIG. 3. Doubling scaling of $S_J(\tau,q)$. (a) $\log_2(\sigma_j) = -1.6 - 0.126(j-1)$, $0 < j \leqslant p$ and $\log_2(\sigma_j) = -2.6 - 0.35(j-1)$, $p < j \leqslant J$ and $p = 9$. The solid lines show the slope of -0.126 and -0.35, respectively. (b) A typical $S_J(\tau,q)$ and the two scaling intervals: $I_1 = \{\tau, \log_2(\tau) \leqslant 7\}$ and $I_2 = \{\tau, \log_2(\tau) > 7\}$. (c) $\zeta(q)$ estimated from scaling interval I_1 ($\bigcirc$) and I_2 ($\square$). They are averaged based on 100 $r_J(t)$ simulated using the σ_j described in (a). The saturation of $\zeta(q) \sim 1$ estimated in I_1 ($\bigcirc$) is an effect of the bounded cascade. The solid line indicates the slope of 0.35.

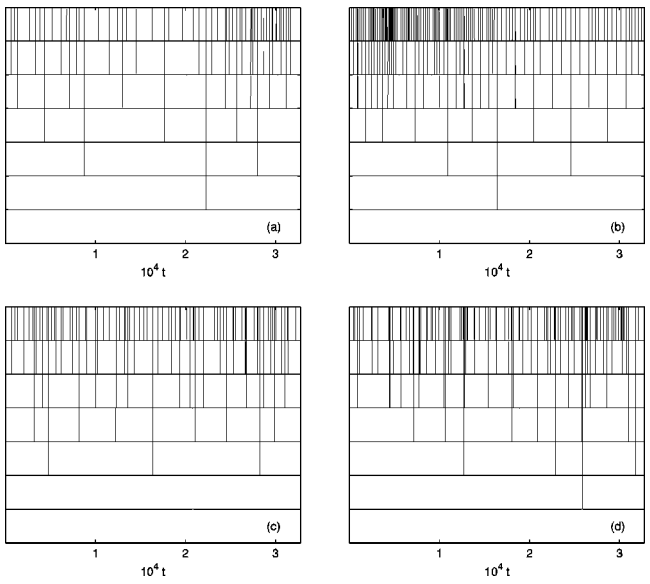

FIG. 4. Representative branching configurations for perturbed cascades. Only the first $j=0,1,...,5$ are shown from bottom to top (the 0th generation is the initial condition): (a) time scale (τ_j) perturbation as described by Eq. (3), (b) mixed dyadic ($\mathbf{C}=2$) and triadic ($\mathbf{C}=3$) branchings, (c) mixed-type branching with 25% of $\{t_k^{(j)}\}$ coincides with those of the dyadic cascade, and (d) mixed-type branching with 0% of $\{t_k^{(j)}\}$ coincides with those of the dyadic cascade.

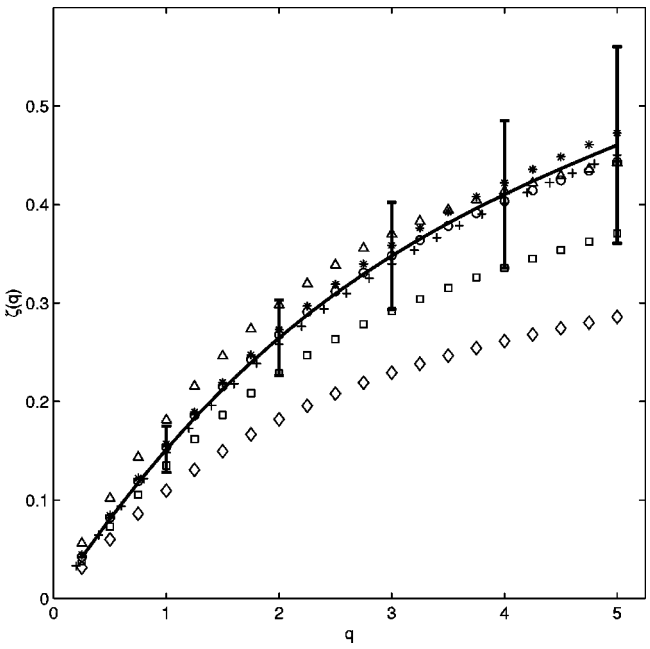

FIG. 5. Scaling in the perturbed cascades with configurations given in Fig. 4. Averaged $\zeta(q)$ based on Fig. 4(a) are shown as $\bigcirc$ for $a=0.4$ and Δ for $a=0.8$ [see Eq. (1)]. Averaged $\zeta(q)$ based on Fig. 4(b) are shown as $\square$ for 80% dyadic, 20% triadic branchings, and $\diamond$ for 50% dyadic, 50% triadic branchings. Averaged $\zeta(q)$ based on Fig. 4(c) is shown as $+$. Averaged $\zeta(q)$ based on Fig. 4d is shown as $\star$. All $\zeta(q)$'s are averaged from 100 samples of $r_J(t)$ using $\log_2(\sigma_j)=-1.6-0.126(j-1)$ and $J=15$. The control with $t_k^{(j)}=k\delta_j$ is shown as the solid line with one standard deviation.

real physical and physiological terms. For example, having $\omega_j(t)$ fluctuating precisely at the dyadic times is certainly an artificial ''constraint.'' To test the robustness of the cascade-generated multifractal and MMFT, the elements (a) and (c) of the above are perturbed. The scaling of the perturbed $r_J(t)$ will be examined by using $\zeta(q)$. In what follows, the dyadic cascade $[t_k(j)=k\delta_j]$ with $\alpha\sim 0.126$ and $\log_2(\sigma_0)\sim -1.6$ estimated from Fig. 1 will be used to generate the *control* in all comparisons.

A. Perturbation of the branching rule

In general, consider $\tau_j=t_{k+1}^{(j)}-t_k^{(j)}$. Figure 4(a) shows the cascade configuration after τ_j is perturbed using

$$\tau_j=(0.5+a\mathbf{U})\,\delta_j\,, \tag{3}$$

where $\mathbf{U}$ is an uniformly distributed random variable in $(-0.5,\ 0.5)$ and $a\in[0,1]$. In the simulation, $\#\{t_k^{(j)}\}=2^j$ is the same as the dyadic cascade. Also, the end points of the parent interval were kept in the offspring's, i.e., $t_{2k}^{(j+1)}=t_k^{(j)}$ [Fig. 4(a)]. This establishes the ''standard'' dyadic configuration except the perturbed interval length. So, $a\neq 0$ describes a random scale scenario. The $\zeta(q)$'s averaged from 100 samples of $r_J(t)$ with $a=0.4,0.8$ show qualitatively similar shapes as the control (Fig. 5). When plotting $\mathcal{S}_J(\tau,q)$ versus $\mathcal{S}_J(\tau,p)$ against each other on the logarithmic scales, which is equivalent to assuming an extended self-similarity in the turbulence analogy of HRV [8], a power law relationship can again be found. The corresponding power law exponent $z_{q,p}$ is given by $\zeta(p)/\zeta(q)$. It is interesting to note that the perturbed $z(p,q)$'s are almost indistinguishable from the control (Fig. 6). In a similar case studied by Falconer, the multifractal spectrum was proven invariant for identically distributed $\mathcal{G}(j)=[f(r_{j+1}(t)/r_j(t)),\mu(\tau_{j+1})/\mu(\tau_j)]$ where $f(\cdot)$ denotes the probability density function and μ is the Lebesgue measure of the Borel sets on the real line [24]. For independent $\omega_j(t)$, the identical $\mathcal{G}(j)$ implies identically distributed $\omega_j(t)$. Arbeiter showed a similar result for the random scale perturbation by using gaussian distribution [25]. The current results are differed from these past studies because the cascade components $\omega_j(t)$ in the bounded cascade are not identically distributed.

In the branching rule perturbation, the intervals in neighboring generations are met at the end points, i.e., for some $\mathbf{C}>0$, the common elements in $\{t_k^{(j)}\}$ and $\{t_{k'}^{(j+1)}\}$:

$$t_{k'}^{(j+1)}=t_k^{(j)} \tag{4}$$

are determined by $k'=\mathbf{C}k$. For example, $\mathbf{C}=2$ applies to the dyadic cascade with $t_{2k}^{(j+1)}=t_k^{(j)}$, $k=1,...,2^j$. Perturbations on $\mathbf{C}$ implies a mixed branching rule where the k', k in Eq. (4) do not commit to any fixed relationship. Different perturbed configurations are considered in Figs. 4(b) and 4(c). Figure 4(b) describes a mixed dyadic and triadic branching rule. In this case, $\mathbf{C}=2$ and $\mathbf{C}=3$ are used in randomly selected intervals with prescribed probabilities (see Fig. 5 caption). Figures 4(c) and 4(d) describe the more general case of

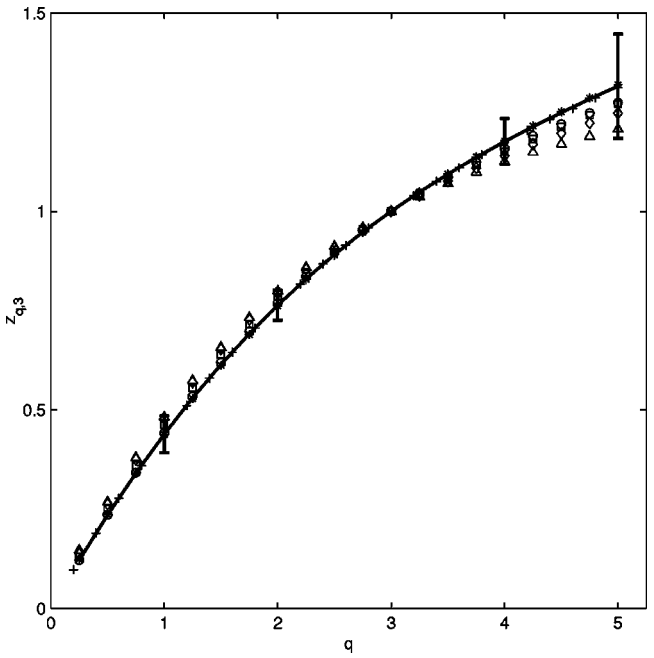

FIG. 6. Normalized $z_{q,3}=\zeta(q)/\zeta(3)$ for all cases shown in Fig. 5. Notice the similar curvatures in all cases.

a random $\mathbf{C}\in\mathbb{N}$ with only the constraint $N_j\leqslant b\times 2^j$, where $N_j=\#\{t_k^{(j)}\}$. In this case, we are interested in perturbing the branching rule from the dyadic case $\mathbf{C}=2$. Shown in Figs. 4(c) and 4(d) are the perturbed configurations with, respectively, 25 and 0 % of the $t_k^{(j)}$ remaining at the branch points of the dyadic cascade ($\mathbf{C}=2$ and $b=3$). Averaged $\zeta(q)<$s in these cases again show similar shapes as the control (Figs. 5 and 6). It is thus evident that a stable multifractal generation persists regardless of the branching rule perturbation, so long as some type of branching mechanism exists to provide the structure for multiplication. Clearly, the branching rule perturbation is not sufficient for MMFT.

B. Perturbation of the product rule

Replacing the multiplicative rule [(c) above] by an additive one can typically lead to the fractal transition reported in HRV under autonomic blockade. Such a perturbation is motivated by the conjecture that feedbacks using additive law are not sufficient to describe the integration of a large number of controls in the autonomic heart rate regulation. It is further motivated by the fact that adding $\omega_j(t)$ with decaying variance on the dyadic tree can lead to monofractal scaling [9]. To perturb the product rule, Eq. (1) is replaced by

$$r_j(t)=r_{j-1}(t)+\omega_j(t) \tag{5}$$

for t in randomly selected subset of $\{t_k^{(j)}\}$. This is conducted by first making a random draw **B** uniformly in [1] to determine such random intervals. The multiplicative rule (1) is applied if the criterion $\mathbf{B}>D$ is satisfied, otherwise, Eq. (5) is used. We tested three cases: uniform perturbation (UP) with a constant $D=D_0$ [Fig. 7(a)], small scale perturbation (SSP) with $D=D_0 j$, where the criterion is less likely passed for large j in the higher generation of the cascade [Fig. 7(b)], and large scale perturbation (LSP) with $D=D_0(J-j)$, where the criterion is less likely passed for small j in the lower generation of the cascade [Fig. 7(c)].

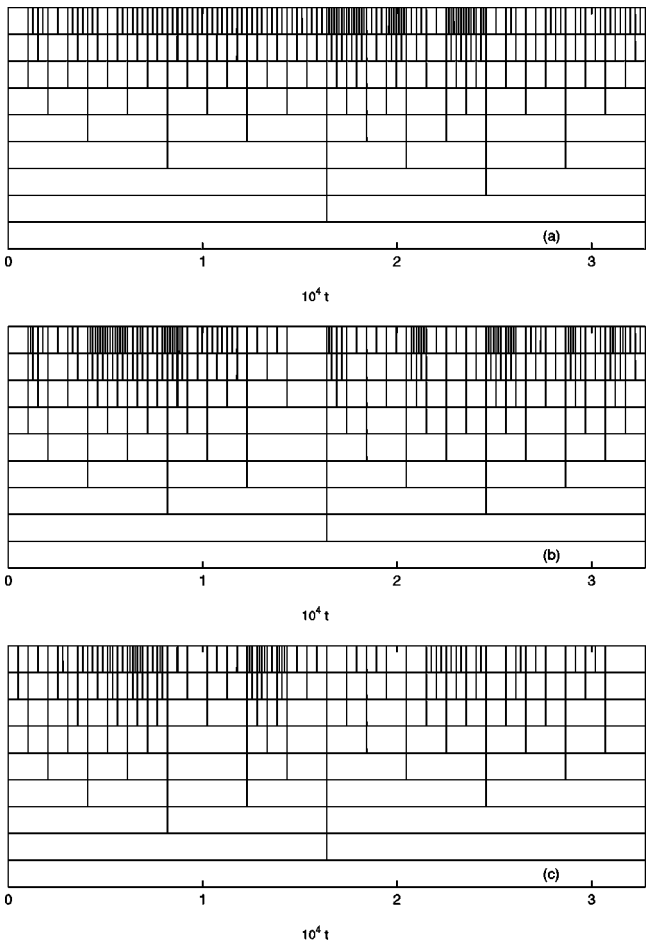

FIG. 7. Representative cascade configurations for perturbed data generation rule. Only the first $j=0,...,8$ generations are shown from bottom to top (the 0th generation is the initial condition). (a) UP, (b) SSP, and (c) LSP; see text for more details. Only the intervals where the multiplicative data generation rule (1) is used are shown.

Since the purpose for the branching rule of the cascade is to provide the structure for the multiplication, it is indirectly perturbed by Eq. (5). As a result, the branching process from one generation to the next can be viewed as containing ''holes'' wherein the product rule does not apply. The $\omega_j(t)$ used in Eq. (5) has mainly the purpose to introduce a noise term in the additive process. Using the same $\omega_j(t)$ helps to make an easier comparison with the control. Other uncorrelated gaussian noise will lead to qualitatively similar results given below.

For UP and SSP, the perturbed $\zeta(q)$ and $z_{q,3}=\zeta(q)/\zeta(3)$ are given in Figs. 8 and 9, respectively. It is evident that a linear trend of $\zeta(q)$ can be developed by the product rule perturbation, which implies MMFT. A closer look indicates the cause of this qualitative change lies in the perturbation of the product rule in the fast time scale. For SSP, a linear $\zeta(q)$ is clearly seen. For UP, increasing D_0 also results in a $\zeta(q)$ of a smaller curvature (more linear). How-

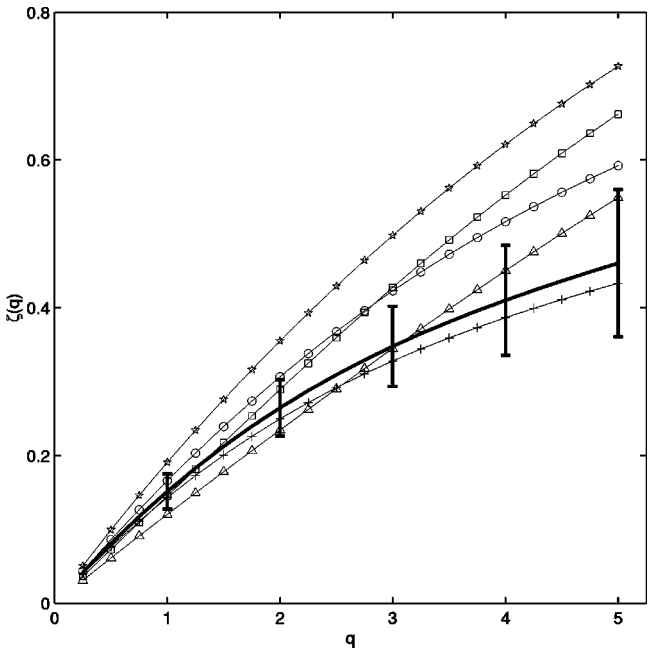

FIG. 8. Scaling in dyadic cascades with perturbed data generation rule described in Fig. 7; see also Eq. (5) in text. (a) $\zeta(q)$ for UP, $D_0=0.05$ (— + —), $D_0=0.3$ (— ⋆ —); $\zeta(q)$ for SSP, $D_0=0.03$ (—Δ—); $\zeta(q)$ for LSP, $D_0=0.03$ (○). The control is shown as the heavy line with one standard deviation. All $\zeta(q)$ are averaged from 100 samples of $r_J(t)$ using $t_k^{(j)}=k\delta_j$, $\log_2(\sigma_j)=-1.6-0.126(j-1)$ and $J=15$. Also shown is the SSP for $D_0=0.03$ (— □ —) using $\log_2(\sigma_j)=-0.25-0.3(j-1)$ and $J=15$.

ever, for LSP, the perturbed $\zeta(q)$ is nonlinear in shape and is qualitatively similar to the control (Fig. 8). The MMFT observed in PNS blockade and minor deviation of the HRV scaling in SNS blockade are consistent to the current finding,

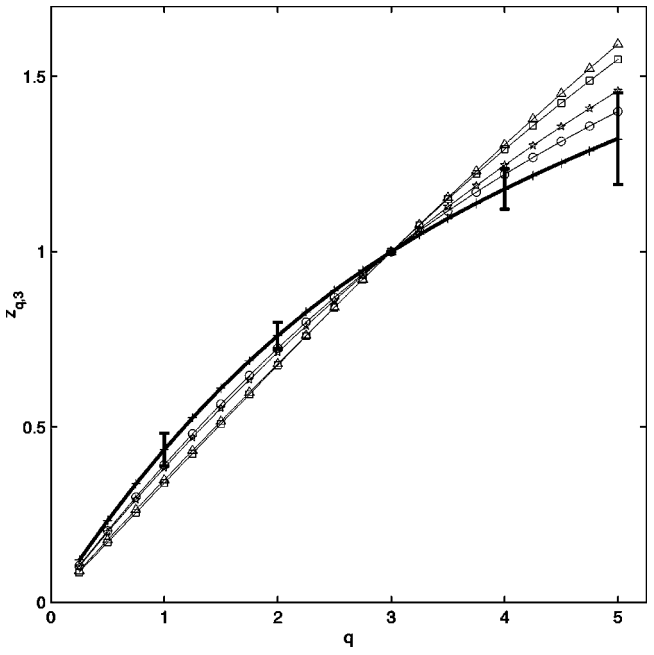

FIG. 9. Normalized $z_{q,3}=\zeta(q)/\zeta(3)$ for all cases shown in Fig. 8. Notice the similar curvatures in all cases.

since PNS and SNS can be characterized by the fast and slow dynamics in the RRi fluctuation [2,4,11]. It implies, in the framework of bounded cascade, that MMFT is likely caused by the perturbation of the data generation rule from a multiplicative to an additive one.

IV. CONCLUSION

In this study, we showed that multifractal scaling is a robust feature and can be generated by using fairly general types of branching process. Qualitatively change can result from perturbing the multiplicative data generation rule into an additive one. MMFT in HRV under PNS blockade was successfully reproduced by this perturbation. We showed in the past that the hierarchical time scale structure of the cascade provides a consistent framework to model the PNS and SNS influences on HRV [10]. As a result, MMFT has also been simulated by ''turning off'' the small time scale generations of the cascade. It was found, on the dyadic times, that the construction of such a truncated cascade mimics that of a Brownian particle's, which is known to exhibit monofractal scaling. The random perturbation studied in Eq. (5) represents a more general scenario leading to MMFT.

In a series of papers, Carlson and Doyle (CD) developed a new theory for the so-called complex system [26]. These authors examined a wide range of physical, biological, and engineering systems and observed that the so-called complex systems are heterogeneous in nature and often exhibit robust feature in the ''design-for'' environment. Such systems can be fragile under unanticipated perturbation. The emphases on the weakness and ''design'' of complex systems separate CD's complexity theory from ideas in statistical physics. The break-down of the robustness was suggested as ''design flaw'' which may be due to a biased training process in the evolution. Introducing heterogeneity to cascade via the branching rule perturbation brings the cascade HRV model closer to CD's complex systems. A robust multifractal generation under the branching rule perturbation suggests a similar type of robustness observed in other complex systems. If this comparison is correct, PNS blockade and its health implication due to ''weakening'' HRV [12,13] should indicate a ''design flaw'' in the human cardiovascular system. We hope the current study could provide the motivation for interdisciplinary efforts to further the understanding of HRV.

ACKNOWLEDGMENTS

This research was supported by the Natural Science and Engineering Research Council of Canada. The author would like to thank Joern Davidson for valuable suggestions.

APPENDIX A

To extract α, we focus on the time averaged statistics since an ensemble average is hard to define in practice. We first define the log increment $y_J(\tau,t)=\log_2[r_J(t+\tau)]-\log_2[r_J(t)]$ for integers τ, t. Assuming dyadic scale and let $\tau=\delta_k$, the pth order moment of y_J $(p>0)$ is given by

$$m_{\delta_k}^{(p)} \sim \frac{1}{N}\sum_t y_J(\delta_k,t)^p = \frac{1}{N}\sum_t \left[\sum_j \rho_j(\delta_k,t)\right]^p, \quad \text{(A1)}$$

where

$$\rho_j(\delta_k,t) = \log_2\left(\frac{\omega_j(t+\delta_k)}{\omega_j(t)}\right). \quad \text{(A2)}$$

Note that $\rho(\delta_k,t)$ can vanish depending on the values of t, δ_k and j. Let $T_k^{(j)}=\{t;\omega_j(t+\delta_k)\neq\omega_j(t)\}$. It can be shown that $T_k^{(j)}$ consists of disjoint segments, each associated with a different $\rho(\delta_k,t)$ value. For a given k, it can be shown $T_k^{(j)}$ for $j\leqslant k$ consists of 2^j-1 such segments, each of which contains δ_k points, and $T_k^{(j)}$ for $j>k$ consists of 2^j-2^{j-k} segments, each of which contains δ_j points. Thus, $|T_k^{(j)}| = (2^j-1)\times\delta_k$ for $j\leqslant k$ and $(2^j-2^{j-k})\times\delta_j$ for $j>k$.

The second moment of the log-increment process is sufficient to provide the first order approximation of α. Since ξ_j's are normal random variables with zero mean and $\langle\xi_j\xi_j\rangle=\delta_{ij}\sigma_j$, the contribution from the jth cascade component to the second moment can be written as

$$\frac{1}{N}\sum_{t=1}^{N}[\rho_j(\delta_k,t)]^2 = \frac{1}{N}\sum_{t\in T_k^{(j)}}[\rho_j(\delta_k,t)]^2 \sim \frac{|T_k^{(j)}|}{N}\left\langle\left[\log_2\left(\frac{1+\xi_j'}{1+\xi_j}\right)\right]^2\right\rangle. \quad \text{(A3)}$$

Substituting Eq. (A3) and $|T_k^{(j)}|$ into (A1) and retaining only the second order terms, one has

$$m_{\delta_k}^{(2)} \sim 2\sum_j \frac{|T_k^{(j)}|}{N}\sigma_j^2 = \frac{\sigma_0^2}{2^{k-1}}\left[\frac{2(1-2^{uk})}{D_1} - \frac{1-2^{-2\alpha k}}{D_2} + (2^k-1)\frac{2^{-2\alpha k}-2^{-2\alpha J}}{D_2}\right], \quad \text{(A4)}$$

where $u=1-2\alpha$, $D_1=1-2^u$, and $D_2=1-2^{-2\alpha}$. It can be seen that $D_1\to-1$, $D_2\to0$ as $\alpha\to0$. Hence, for small α, $D_2/D_1\sim0$. Now, assuming $2^J\gg\delta_k\gg1$, it can be shown $m_{\delta_k}^{(2)}\sim\delta_k^{2\alpha}$, which implies α can be estimated by linear regression in the middle range scales.

APPENDIX B

The power law $\mathcal{S}_J(\tau,q)$ of the dyadic bounded cascade has been shown in the past based on the variance law $\sigma_j = \sigma_0 2^{-\alpha(j-1)}$ [8]. In general, it can be written

$$\mathcal{S}_J(\tau,q) = \sum_{n=0}^{J-\nu-1}\mathcal{P}_n\langle|\mathcal{D}\omega_n|^q\rangle, \quad \text{(B1)}$$

where $\mathcal{P}_n=2^n\tau/(2^J-\tau)$, $\tau=2^\nu$ and $\langle|\mathcal{D}\omega_n|^q\rangle$ is defined by Eq. (2). The power law scaling in Eq. (B1) only holds for large τ [9]. The purpose of this Appendix is to show that a second scaling will emerge in small τ if the variance σ_j decays sufficiently fast. As a result, if there are two decay rates for σ_j, the dyadic cascade is able to exhibit double scaling observed in *some* experimental data [7].

Considering $\sigma_j\ll0$ for $j\geqslant p$ and $1<p<J$, it can be shown that

$$|\mathcal{D}\omega_n|^q \sim \left|\prod_{j=1}^{p-1}\omega_j\right|^q\left|\sum_{j=n+1}^{J}\Delta\xi_j\right|^q. \quad \text{(B2)}$$

For independent ω_j's,

$$\left\langle\left|\prod_{j=1}^{p-1}\omega_j\right|^q\right\rangle \sim \sigma_0^{(p-1)q}2^{-(p-1)(p-2)\alpha q/2} \quad \text{(B3)}$$

and

$$\left\langle\left|\sum_{j=n+1}^{J}\Delta\xi_j\right|^q\right\rangle \sim 2^{q/2}\sigma_0^q\left[\frac{2^{-2\alpha n}-2^{-2\alpha J}}{1-2^{-2\alpha}}\right]^{q/2}. \quad \text{(B4)}$$

Taking the statistical average of Eq. (B2) with Eqs. (B3) and (B4), and substituting the result back to Eq. (B1) yield

$$S_J(\rho,q) \sim G(p,q,\alpha)(2^{(J-p+1)(1-\alpha q)}\tau^{\alpha q}-\tau), \quad \text{(B5)}$$

where

$$G(p,q,\alpha) = \sigma_0^{pq}\frac{2^{[q-2p+2-p(p-1)\alpha q]/2}}{(1-2^{-2\alpha})^{q/2}(2^{1-\alpha q}-1)2^J}.$$

In Eq. (B5), the assumption $2^J\gg\tau$ was used since we are interested in finding the scaling in small τ. Note that depending on the p value, the exponent of the first term in Eq. (B5), $(J-p+1)(1-\alpha q)$, varies from the largest $(J-1)(1-\alpha q)$ to the smallest $2(1-\alpha q)$. For p lies in the middle range, say $p\sim J/2$, $(J-p+1)(1-\alpha q)\sim(1+J/2)(1-\alpha q)$. Using $J=15$ ($\sim$30 000 beats), the factor multiplied to $\tau^{\alpha q}$ is approximately $2^8(1-\alpha q)$. Thus, the first term in Eq. (B5) can be significantly larger and for $q<q_*$, where $1=\alpha q_*$, $S_J(\tau,q)\sim\tau^{\alpha q}$.

[1] G. C. Butler, Y. Yamamoto, and R. L. Hugson, J. Clin. Pharmacol. **34**, 558 (1994); Am. J. Physiol. Regul. Integr. Comp. Physiol. **267**, R26 (1994).

[2] Task force of the ESC and NASPE, Eur. Heart J. **17**, 354 (1996).

[3] P. Ch. Ivanov, A. Bunde, L. A. N. Amaral, J. Fritsch-Yelle, R. M. Baevsky, S. Havlin, H. E. Stanley, and A. L. Goldberger, Europhys. Lett. **48**, 594 (1999).

[4] F. Lombardi, A. Malliani, M. Pagani, and S. Cerutti, Cardiovasc. Res. **32**, 208 (1996).

[5] M. Kohayashi and T. Musha, IEEE Trans. Biomed. Eng. **29**, 456 (1982).

[6] J. T. Bigger *et al.*, Circulation **93**, 2142 (1996).

[7] C-K. Peng, S. Havlin, H. E. Stanley, and A. L. Goldberger, Chaos **5**, 82 (1995).
[8] P. CH. Ivanov, L. A. N. Amaral, A. L. Goldberger, S. Havlin, M. G. Rosenblum, Z. R. Struzik, and H. E. Stanley, Nature (London) **399**, 461 (1999).
[9] D. C. Lin and R. L. Hughson, Phys. Rev. Lett. **86**, 1650 (2001); D. C. Lin and R. L. Hughson, IEEE Trans. Biomed. Eng. **49**, 97 (2002).
[10] D. C. Lin, Fractals (to be published).
[11] L. A. N. Amaral, P. Ch. Ivanov, N. Aoyagi, I. Hidaka, S. Tomono, A. L. Goldberger, H. E. Stanley, and Y. Yamamoto, Phys. Rev. Lett. **86**, 6026 (2001).
[12] Y. Yamamoto and R. L. Hughson, Am. J. Physiol. Regul. Integr. Comp. Physiol. **266**, R40 (1994); Y. Yamamoto, Y. Nakamura, H. Sato, M. Yamamoto, K. Kato, and R. L. Hughson, Am. J. Physiol. **269**, R830 (1995).
[13] G. C. Butler, S. Ando, and J. S. Floras, Clin. Sci. **92**, 543 (1997).
[14] J. O. Fortrat, D. Sigaudo, R. L. Hughson, A. Maillet, Y. Yamamoto, and C. Gharib, Auton. Neurosci. **86**, 192 (2001).
[15] C. Meneveau and K. R. Sreenivasan, J. Fluid Mech. **224**, 429 (1991).
[16] R. H. Riedi, M. S. Crouse, V. Ribiero, and R. G. Baraniuk, IEEE Trans. Inf. Theory **45**, 992 (1999).
[17] J. F. Muzy, J. Delour, and E. Bacry, Eur. Phys. J. B **17**, 537 (2000).
[18] R. Holley and E. C. Waymire, Ann. Appl. Probab. **2**, 819 (1992).
[19] A. Marshak, A. Davis, R. Cahalan, and W. Wiscombe, Phys. Rev. E **49**, 55 (1994).
[20] A. L. Goldberger, L. A. N. Amaral, L. Glass, J. M. Hausdorff, P. Ch. Ivanov, R. G. Mark, J. E. Mietus, G. B. Moody, C.-K. Peng, and H. E. Stanley, Circulation **101**, e215 (2000).
[21] U. Frisch, *Turbulence: The Legacy of A. N. Kolmogorov* (Cambridge University Press, Cambridge, 1995).
[22] J. F. Muzy, E. Bacry, and A. Arneodo, Phys. Rev. E **47**, 875 (1993).
[23] K. Falconer, *Fractal Geometry, Mathematical Foundations and Applications*, 1st ed. (John Wiley & Sons, New York, 1990).
[24] K. Falconer, J. Theor. Prob. **7**, 681 (1994).
[25] M. Arbeiter, Stoch. Stoch. Rep. **39**, 195 (1992).
[26] J. M. Carlson and J. Doyle, Phys. Rev. E **60**, 1412 (1999).